ЖЭТФ, 2015, том 148, вып. 6 (12), стр. 1059–1067

MULTIPHOTON DYNAMICS OF QUTRITS IN THE ULTRASTRONG COUPLING REGIME WITH A QUANTIZED PHOTONIC FIELD

H. K. Avetissian [a]*, ***A. K. Avetissian*** [a], ***G. F. Mkrtchian*** [a], ***O. V. Kibis*** [b]

[a] *Center of Strong Fields Physics, Yerevan State University*
0025, Yerevan, Armenia

[b] *Department of Applied and Theoretical Physics, Novosibirsk State Technical University*
630073, Novosibirsk, Russia

Received June 10, 2015

Multiphoton resonant excitation of a three-state quantum system (a qutrit) with a single-mode photonic field is considered in the ultrastrong coupling regime, when the qutrit–photonic field coupling rate is comparable to appreciable fractions of the photon frequency. For ultrastrong couplings, the obtained solutions of the Schrödinger equation reveal multiphoton Rabi oscillations in qutrits with the interference effects leading to the collapse and revival of atomic excitation probabilities at the direct multiphoton resonant transitions.

DOI: 10.7868/S0044451015120019

1. INTRODUCTION

The behavior of quantum systems with a few energy levels in a quantized photonic field and the evolution of resonant transitions with coherent dynamic effects in diverse interaction regimes are the subject of intensive investigations of the last two decades. Besides the natural atoms, such quantum systems include a large class of artificial atoms with different elements and configurations of cavity/circuit quantum electrodynamics (QED), which exhibit various coherent effects with specific quantum dynamics, like the collapse and revival of atomic inversion population with Rabi oscillations, the formation of photon entangled states, squeezing, manifestation of the purely quantum statistics of light, and so on [1–3]. Among these quantum systems, the two-level and the three-level systems — so called qubits or qutrits — are of great importance for modern quantum physics. In the case of two-level quantum systems, there is a well-known model, the so-called Jaynes–Cummings (JC) model [4, 5], which describes the resonant interaction of such systems with strong and quantized radiation fields, as well as the single-photon interaction processes with the vacuum fluctuations in quantum microcavities. The coupling of such atomic systems to quantum radiation modes in the simple scheme of a quantum harmonic oscillator have important applications in many significant fields of contemporary physics, specifically, in quantum optics and informatics [6–8] and in condensed matter physics [9–11].

Regarding the three-state quantum systems, qutrits, we note their role in coherent manipulation with two-level atoms (qubits) and, in general, quantum systems via an additional third quantum state, which allows revealing a large class of coherent interference effects, as well as the use of the qutrits in composing of many quantum protocols and in storing quantum information [12]. The various cases of three-state atoms, such as the ladder (Ξ), the vee (V), and the lambda (Λ), coupled to a quantized field have been treated by many authors (see [1, 2] and the references therein). As has been shown in Refs. [13, 14], there is a three-state configuration — which can be referred to as the Γ configuration — where multiphoton transitions in the quantum dynamics of the system subjected to a classical strong radiation field are very effective compared to the Ξ, V, and Λ configurations. The configuration inverse to Γ is the L configuration, which is unitarily equivalent to the polar-Λ configuration (see below). The aforementioned investigations [13, 14] have been carried out for a given classical radiation field. It is of interest to study the interaction of a polar-Λ/V atom with a single-mode quantized radiation field, where new pure quantum multiphoton effects are expected.

*E-mail: avetissian@ysu.am

Thanks to the recent achievements in cavity/circuit QED [15], it has become possible to achieve interaction-dominated regimes in which multiphoton effects are expected. This occurs in the ultrastrong coupling regime when the atom–photon coupling rate is comparable to appreciable fractions of the oscillator frequency [15]. There, nonresonant terms of the interaction Hamiltonian, usually accounted for in external strong fields, become relevant even at the interaction with vacuum fluctuations. In this regime, new nonlinear and multiphoton effects [16–22] are predicted that are not present in the weak-or strong-coupling regimes [23]. In particular, the ground state is predicted to be a squeezed vacuum containing a finite number of virtual photons [16]. Real photons can be created from the vacuum fluctuations via the dynamical Casimir [17] or other effects [18]. In the ultrastrong coupling regime, nonclassical photonic states including squeezed states, Schrödinger-cat states, and entangled states can be created [19]. The electron coupling to photons in the field-dressed nanostructures can result in the ground electron–photon state with a nonzero electric current [20]. The interaction of the nanostructure with vacuum fluctuations of an optical cavity can open gaps within the valence band of a semiconductor [21]. At the breaking of the inversion symmetry in two-level systems, it is possible to realize Rabi oscillations, the collapse and revival of the initial population with the periodic multiphoton exchange between the atom and the radiation field [22]. Hence, investigating new systems with effective multiphoton transitions in the quantized photonic field at ultrastrong light–matter couplings is of interest.

In this paper, we consider the multiphoton resonant interaction of an artificial qutrit atom with a quantized radiation field. To be specific, we assume the qutrit to be in a polar-Λ configuration, in which diagonal matrix elements of the dipole moment operator have nonzero values for two lower states. The results can also be applied to the polar-V configuration. We consider direct multiphoton resonant transitions in the ultrastrong coupling regime. We study the effect of permanent dipole moments of stationary states on the quantum dynamics of a three-level system interacting with a quantized radiation field. In particular, we consider the eigenstates and eigenenergies of the generalized JC Hamiltonian, and the dynamics of Rabi oscillations, collapse, and revival. It is shown that due to the permanent dipole moments, direct multiphoton transitions occur, and, as a consequence, Rabi oscillations arise with a periodic exchange of several photons between the emitter and the radiation (boson) field. The quantum dynamics of the considered system is investigated using the multiphoton resonant approximation. As a specific example, we do numerical calculations for an artificial atom realized via a three-Josephson-junction loop.

This paper is organized as follows. In Sec. 2, the model Hamiltonian is introduced and diagonalized in the scope of the multiphoton resonant approximation. In Sec. 3, we consider temporal quantum dynamics of the considered system and present the corresponding numerical simulations. Finally, conclusions are given in Sec. 4.

2. BASIC HAMILTONIAN AND THE RESONANT APPROXIMATION

We consider a three-state quantum system — qutrit — interacting with the single-mode radiation field of a frequency ω. The system is schematically illustrated in Fig. 1. We assume the qutrit to be in the polar-Λ configuration, in which two lower states $|g_1\rangle$ and $|g_2\rangle$ with permanent dipole moments are coupled to a single upper state $|e\rangle$. An other possible three-level scheme is shown in the lower part of Fig. 1, referred to as the L configuration. In that case, the upper state is coupled to a lower state, which is in turn

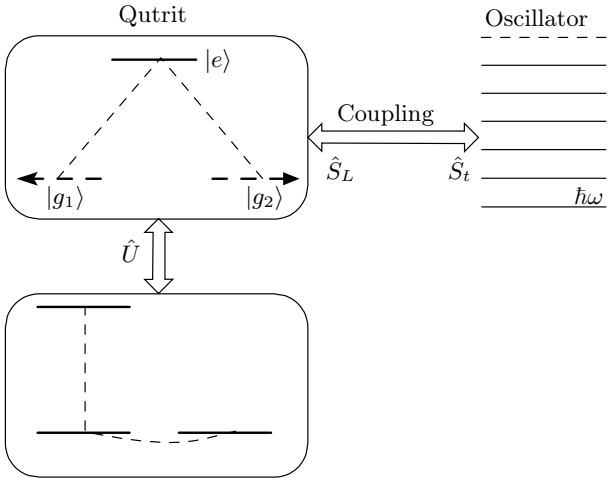

Fig. 1. Schematic of the system under consideration. A qutrit in the polar-Λ configuration is coupled to a quantized single-mode field, represented as a harmonic oscillator with the characteristic frequency ω. Two lower states $|g_1\rangle$ and $|g_2\rangle$ with the permanent dipole moments are coupled to a single upper level $|e\rangle$. The considered configuration is unitarily equivalent to the L configuration shown in the lower part of the diagram. In this case, the upper level is coupled to the lower level, which in turn is coupled to an adjacent level

above coupled to an adjacent state. For the L, configuration the permanent dipole moment is zero for stationary states. The polar-Λ configuration is unitarily equivalent to the L configuration. A more in-depth discussion of this point can be found in the Appendix. The above qutrit configuration can be realized, for example, in a symmetric double-well potential for solid-state semiconductor or superconductor systems [24]. In particular, the effective potential landscape reduces to a double-well potential for the superconducting quantum interference device loop [25] and the three-Josephson-junction loop [26, 27].

We assume a coupling to a bosonic field, with the transition selection rules equivalent to the ones for the electric-dipole transitions in usual atoms. For the artificial atom based on the superconducting quantum circuit, the eigenstates involve a macroscopic number of electrons. However, as was shown in Ref. [28], the optical selection rules of microwave-assisted transitions in a flux qubit superconducting quantum circuit are the same as for the electric-dipole transitions in usual atoms when the effective potential landscape reduces to a symmetric double-well potential.

Hence, in the basis

$$|g_1\rangle = \begin{pmatrix} 1 \\ 0 \\ 0 \end{pmatrix}, \quad |g_2\rangle = \begin{pmatrix} 0 \\ 1 \\ 0 \end{pmatrix}, \quad |e\rangle = \begin{pmatrix} 0 \\ 0 \\ 1 \end{pmatrix}, \tag{1}$$

the Hamiltonian for the polar-Λ system coupled to a bosonic field can be represented in the form

$$\widehat{H} = \hbar\omega\left(\widehat{a}^\dagger\widehat{a} + \frac{1}{2}\right) + \widehat{H}_\Lambda + \hbar\left(\mu\widehat{S}_L + \lambda\widehat{S}_t\right)\left(\widehat{a}^\dagger + \widehat{a}\right). \tag{2}$$

The first term in Eq. (2) corresponds to the free harmonic oscillator of the frequency ω (a single-mode radiation field). The second term,

$$\widehat{H}_\Lambda = \begin{pmatrix} \varepsilon_g & \Delta & 0 \\ \Delta & \varepsilon_g & 0 \\ 0 & 0 & \varepsilon_e \end{pmatrix}, \tag{3}$$

corresponds to the three-level system. Here, the nondiagonal elements Δ describe transitions between lower-lying states (tunnel transitions). The last term in Eq. (2) gives the interaction between the single-mode radiation field and the qutrit. Creation and annihilation operators $\widehat{a}^\dagger$ and $\widehat{a}$, satisfy the bosonic commutation rules. The operator

$$\widehat{S}_L = -|g_1\rangle\ \langle g_1| + |g_2\rangle\ \langle g_2| = \begin{pmatrix} -1 & 0 & 0 \\ 0 & 1 & 0 \\ 0 & 0 & 0 \end{pmatrix} \tag{4}$$

is the result of the permanent dipole moments in states of indefinite parity. The term with $\widehat{S}_L$ in Eq. (2) describes the self-energy oscillating levels and is responsible for the direct multiphoton resonances [13, 14]. The operator

$$\widehat{S}_t = |g_1\rangle\langle e| - |g_2\rangle\langle e| + \text{H.c.} = \begin{pmatrix} 0 & 0 & 1 \\ 0 & 0 & -1 \\ 1 & -1 & 0 \end{pmatrix} \tag{5}$$

describes transitions between excited and lower-lying states. At $\mu = 0$, we have the usual Hamiltonian for the Λ model. At $\lambda = 0$, the excited state decouples, and after unitary transformation (A.5) (see Appendix), we obtain the usual Hamiltonian for the JC model (also including counter-rotating terms) with the coupling $\hbar\mu$ and atomic energy 2Δ. Hence, to emphasize the three-state structure in this paper, we consider the case $|\Delta| \ll \hbar\omega < \varepsilon_e - \varepsilon_g$.

Here, we consider interaction of an artificial atom with a single mode of the resonator. In general, the resonator supports other eigenmodes. Usually, in cavity and circuit QED setups, one can engineer the device to limit the spectral proximity of and couplings to higher modes of the cavity [29, 30]. In many cases [15–22], it is sufficient to characterize the behavior of the circuit only in the vicinity of the fundamental frequency, where the general Hamiltonian reduces to the single-mode Hamiltonian. This is justified especially at the resonant interaction, where the single-mode approximation provides a sufficient understanding of the quantum dynamics. The higher modes of the cavity and other levels of the artificial atom cause the AC–Stark shift of the considered levels, which can be taken into account for a specific system by the calibration of transition frequencies.

We first diagonalize Hamiltonian (2) for moderately strong couplings, which is straightforward in the resonant case. For $\Delta = 0$, Hamiltonian (2) can be rewritten in the form

$$\widehat{H} = \widehat{H}_0 + \widehat{V}, \tag{6}$$

where

$$\widehat{H}_0 = \widehat{H}_{osc} \otimes \widehat{P}_e + \widehat{H}_- \otimes \widehat{P}_{g_1} + \widehat{H}_+ \otimes \widehat{P}_{g_2} \tag{7}$$

represents three noncoupled oscillators. Here, $\widehat{P}_{g_1} = |g_1\rangle\langle g_1|$, $\widehat{P}_{g_2} = |g_2\rangle\langle g_2|$, and $\widehat{P}_e = |e\rangle\langle e|$ are projection operators. The excited state is associated with the normal oscillator with the Hamiltonian

$$\widehat{H}_{osc} = \hbar\omega\left(\widehat{a}^\dagger\widehat{a} + \frac{1}{2}\right) + \varepsilon_e, \tag{8}$$

and the other two are associated with position-displaced oscillators

$$\widehat{H}_- = \hbar\omega\left(\widehat{a}^\dagger\widehat{a} + \frac{1}{2}\right) + \varepsilon_g - \hbar\mu\left(\widehat{a}^\dagger + \widehat{a}\right), \tag{9}$$

$$\widehat{H}_+ = \hbar\omega\left(\widehat{a}^\dagger\widehat{a} + \frac{1}{2}\right) + \varepsilon_g + \hbar\mu\left(\widehat{a}^\dagger + \widehat{a}\right). \tag{10}$$

The interaction part

$$\widehat{V} = \hbar\lambda\widehat{S}_t\left(\widehat{a}^\dagger + \widehat{a}\right) \tag{11}$$

in Eq. (6) couples $\widehat{H}_{osc}$ to $\widehat{H}_-$ and $\widehat{H}_+$. Hamiltonians (8), (9), and (10) admit exact diagonalization. It is easy to see that the corresponding eigenstates are

$$\begin{aligned} &|e, N^{(osc)}\rangle \equiv |e\rangle \otimes |N\rangle, \\ &|g_1, N^{(-)}\rangle \equiv |g_1\rangle \otimes \exp\left[\frac{\mu}{\omega}(\hat{a}^\dagger - \hat{a})\right]|N\rangle, \\ &|g_2, N^{(+)}\rangle \equiv |g_2\rangle \otimes \exp\left[-\frac{\mu}{\omega}(\hat{a}^\dagger - \hat{a})\right]|N\rangle, \end{aligned} \tag{12}$$

with the energies

$$\begin{aligned} E_{eN} &= \varepsilon_e + \hbar\omega\left(N + \frac{1}{2}\right), \\ E_{g_1N} &= E_{g_2N} = \varepsilon_g + \hbar\omega\left(N + \frac{1}{2}\right) - \hbar\frac{\mu^2}{\omega}. \end{aligned} \tag{13}$$

Here, $D(\alpha) = \exp[\alpha(\hat{a}^\dagger - \hat{a})]$ is the displacement operator, and the quantum number is $N = 0, 1, \ldots$ The states $|N^{(+)}\rangle$, $|N^{(-)}\rangle$ are position-displaced Fock states:

$$\begin{aligned} |N^{(+)}\rangle &= \exp\left[-\frac{\mu}{\omega}(\hat{a}^\dagger - \hat{a})\right]|N\rangle = \\ &= \sum_M I_{N,M}\left(\frac{\mu^2}{\omega^2}\right)|M\rangle, \\ |N^{(-)}\rangle &= \exp\left[(\mu/\omega)(\hat{a}^\dagger - \hat{a})\right]|N\rangle = \\ &= \sum_M I_{M,N}\left(\frac{\mu^2}{\omega^2}\right)|M\rangle, \end{aligned} \tag{14}$$

where $I_{N,M}(\alpha)$ is the Laguerre function defined in terms of generalized Laguerre polynomials $L_n^l(\alpha)$ as

$$\begin{aligned} I_{s,s'}(\alpha) &= \sqrt{\frac{s'!}{s!}}\exp\left(-\frac{\alpha}{2}\right)\alpha^{(s-s')2}L_{s'}^{s-s'}(\alpha) = \\ &= (-1)^{s-s'}I_{s',s}(\alpha), \\ L_n^l(\alpha) &= \frac{1}{n!}e^\alpha\alpha^{-l}\frac{d^n}{d\alpha^n}\left(e^{-\alpha}\alpha^{n+l}\right). \end{aligned} \tag{15}$$

In particular, $|0^{(+)}\rangle$ and $|0^{(-)}\rangle$ are the Glauber or coherent states with the mean number of photons μ^2/ω^2. Thus, we have three ladders, two of them are crossed, and one ladder shifted by the energy

$$\hbar\omega_{eg} = \hbar\left(\omega_0 + \mu^2/\omega\right), \tag{16}$$

where $\omega_0 = (\varepsilon_e - \varepsilon_g)/\hbar$. The coupling term (11), $\widehat{V} \sim \widehat{S}_t$, induces transitions between these manifolds. At the resonance,

$$\omega n - \omega_{eg} = \delta_n, \quad |\delta_n| \ll \omega, \tag{17}$$

where $n = 1, 2, \ldots$, the equidistant ladders are crossed, $E_{eN} \approx E_{g_1N+n} = E_{g_2N+n}$, and the energy levels of the upper harmonic oscillators starting from the ground state are nearly threefold degenerate. The coupling (11) removes this degeneracy, leading to "qutrit–photon" entangled states. The splitting of levels is defined by the vacuum multiphoton Rabi frequency. In this case, we should apply the secular perturbation theory. Taking into account that

$$\langle g_1, N^{(-)}|\widehat{V}|e, N-n\rangle = (-1)^n\langle g_2, N^{(+)}|\widehat{V}|e, N-n\rangle,$$

and seeking the solution in the form

$$\begin{aligned} |\alpha, N\rangle = C_{g_1}^{(\alpha)}|g_1, N^{(-)}\rangle + C_{g_2}^{(\alpha)}|g_2, N^{(+)}\rangle + \\ + C_e^{(\alpha)}|e, N-n\rangle, \end{aligned} \tag{18}$$

we obtain the eigenenergies

$$E_{1,N} = \varepsilon_g + \hbar\omega\left(N + \frac{1}{2}\right) - \hbar\frac{\mu^2}{\omega}, \tag{19}$$

$$E_{2,N} = E_{1,N} + \sqrt{2}\,|V_N(n)|, \tag{20}$$

$$E_{3,N} = E_{1,N} - \sqrt{2}\,|V_N(n)| \tag{21}$$

and corresponding eigenstates

$$|1, N\rangle = \frac{1}{\sqrt{2}}\left(|g_1, N^{(-)}\rangle + (-1)^{n+1}|g_2, N^{(+)}\rangle\right), \tag{22}$$

$$\begin{aligned} |2, N\rangle = \frac{1}{2}|g_1, N^{(-)}\rangle + (-1)^n\frac{1}{2}|g_2, N^{(+)}\rangle + \\ + \frac{\exp(-i\varphi_{V_N})}{\sqrt{2}}|e, N-n\rangle, \end{aligned} \tag{23}$$

$$\begin{aligned} |3, N\rangle = \frac{1}{2}|g_1, N^{(-)}\rangle + (-1)^n\frac{1}{2}|g_2, N^{(+)}\rangle - \\ - \frac{\exp(-i\varphi_{V_N})}{\sqrt{2}}|e, N-n\rangle. \end{aligned} \tag{24}$$

In Eqs. (20)–(24), the transition matrix element is

$$V_N(n) \equiv \langle g_1, N^{(-)}|\widehat{V}|e, N-n\rangle = \\ = \hbar\lambda\sqrt{N-n}I_{N-n-1,N}\left(\frac{\mu^2}{\omega^2}\right) + \\ + \hbar\lambda\sqrt{N-n+1}I_{N-n+1,N}\left(\frac{\mu^2}{\omega^2}\right), \quad (25)$$

and $\varphi_{V_N} = \arg[V_N(n)]$. Thus, starting from the level $N = n$, we have qutrit–photon entangled states (23) and (24), while for $N = 0, 1, \ldots, n-1$, we have twofold degenerate eigenenergies E_{1N} with the states $|g_1, N^{(-)}\rangle$ and $|g_2, N^{(+)}\rangle$. At $\mu = 0$, similarly to the conventional JC model, there is a selection rule: $V_N(n) \neq 0$ only for $n = \pm 1$. In this case, only one photon Rabi oscillation occurs. In our model with $\mu \neq 0$, there are transitions with arbitrary n, giving rise to multiphoton coherent transitions. Solutions (22)–(24) are valid close to the multiphoton resonance $\omega_{eg} \approx n\omega$ and at weak coupling:

$$|V_N(n)| \ll \hbar\omega. \quad (26)$$

3. MULTIPHOTON RABI OSCILLATIONS IN THE ULTRASTRONG COUPLING REGIME

In this section, we consider temporal evolution of the qutrit–photonic-field system. This is of particular interest for applications in quantum information processing. We also present numerical solutions of the time-dependent Schrödinger equation with the full Hamiltonian (2).

We first consider the quantum dynamics of the qutrit coupled to a photonic field starting from an initial state that is not an eigenstate of Hamiltonian (2). For an arbitrary initial state $|\Psi_0\rangle$ of the system, the state vector for times $t > 0$ is given by the expansion over the basis obtained above:

$$|\Psi(t)\rangle = \sum_{N=0}^{n-1}\langle g_1, N^{(-)}||\Psi_0\rangle \times \\ \times \exp\left(-\frac{i}{\hbar}E_{g_1N}t\right)|g_1, N^{(-)}\rangle + \\ + \sum_{N=0}^{n-1}\langle g_2, N^{(+)}||\Psi_0\rangle \exp\left(-\frac{i}{\hbar}E_{g_2N}t\right)|g_2, N^{(+)}\rangle + \\ + \sum_{\alpha=1}^{3}\sum_{N=n}^{\infty}\langle \alpha, N||\Psi_0\rangle \exp\left(-\frac{i}{\hbar}E_{\alpha,N}t\right)|\alpha, N\rangle. \quad (27)$$

To be specific, we consider two common initial conditions for the photonic field: the Fock state and the coherent state. We calculate the time dependence of the three-level system population inversion

$$W_n(t) = \langle\Psi(t)|\widehat{\Sigma}_z|\Psi(t)\rangle \quad (28)$$

at the exact n-photon resonance (17), where

$$\widehat{\Sigma}_z = \begin{pmatrix} -1 & 0 & 0 \\ 0 & -1 & 0 \\ 0 & 0 & 1 \end{pmatrix}. \quad (29)$$

For the field in the vacuum state and the qutrit in the excited state $|\Psi_0\rangle = |e, 0\rangle$, it follows from Eqs. (22)–(24), and (27) that

$$|\Psi(t)\rangle = \frac{\exp(i\varphi_{V_n})}{\sqrt{2}}\exp\left(-\frac{i}{\hbar}E_{2,n}t\right)\times \\ \times\{|2, n\rangle - \exp[i\Omega_n(n)t]|3, n\rangle\}, \quad (30)$$

where

$$\Omega_N(n) = \frac{2\sqrt{2}|V_N(n)|}{\hbar} \quad (31)$$

is the multiphoton vacuum Rabi frequency. From Eqs. (28)–(30), we obtain the population inversion

$$W_n(t) = \cos(\Omega_n(n)t), \quad (32)$$

which corresponds to Rabi oscillations with a periodic exchange of n photons between the qutrit and the radiation field.

We next turn to the case where the qutrit begins in an excited state, with the photonic field prepared in a coherent state with a mean photon number $\overline{N}$:

$$|\Psi_0\rangle = |e\rangle \otimes \exp\left[\sqrt{\overline{N}}(\hat{a}^\dagger - \hat{a})\right]|0\rangle. \quad (33)$$

Taking Eqs. (27) and (33) into account, we obtain the wave function

$$|\Psi(t)\rangle = \sum_{N=n}^{\infty}\frac{\exp(i\varphi_{V_N})}{\sqrt{2}}I_{N-n,0}\left(\overline{N}\right)\times \\ \times\left[\exp\left(-\frac{i}{\hbar}E_{2,N}t\right)|2, N\rangle - \right. \\ \left. - \exp\left(-\frac{i}{\hbar}E_{3,N}t\right)|3, N\rangle\right], \quad (34)$$

which for population inversion (28) gives

$$W_n(t) = \sum_{N=0}^{\infty}\frac{e^{-\overline{N}}}{N!}\overline{N}^N\cos[\Omega_{N+n}(n)t]. \quad (35)$$

In this case, we have superposition of Rabi oscillations with the amplitudes given by the Poisson distribution $P_N = e^{-\overline{N}}\overline{N}^N/N!$. As a consequence, we have the collapse and revival phenomena of the multiphoton Rabi

oscillations. There are dominant frequencies in Eq. (35) as a result of the spread of probabilities about $\overline{N}$ for photon numbers in the range $\overline{N} \pm \sqrt{\overline{N}}$. When these terms oscillate out of phase with each other in sum (35), their cancelation is expected (the collapse of Rabi oscillations). Hence, for large photon numbers $\overline{N} \gg \sqrt{\overline{N}}$, the collapse time can be estimated as

$$t_{\mathrm{c}}^{(n)} \approx \frac{\pi}{2\sqrt{\overline{N}}} \left(\frac{\partial \Omega_N (n)}{\partial N} \right)^{-1}. \qquad (36)$$

Recalling Eq. (25), we see that in contrast to the conventional JC model, collapse time (36) strongly depends on the mean photon number.

We now consider numerical solutions of the time-dependent Schrödinger equation with the full Hamiltonian (2) in the Fock basis:

$$|\Psi (t)\rangle = \sum_{\sigma=g_1,g_2,e} \sum_{N=0}^{N_{max}} C_{\sigma,N} (t) |\sigma\rangle \otimes |N\rangle. \qquad (37)$$

The set of equations for the probability amplitudes $C_{\sigma,N} (t)$ has been solved using a standard fourth-order Runge–Kutta algorithm, considering up to $N_{max} = 200$ excitations. The Schrödinger equation with the full Hamiltonian (2) was solved numerically with the parameters corresponding to the setup considered in [4] (see Appendix). The tunneling parameter and the ratio of the permanent dipole moment to the transition one are taken to be $\omega_0/\Delta \approx 25$ and $|\mu/\lambda| \approx 5.75$.

To show the periodic multiphoton exchange between the qutrit and the radiation field, we have calculated population inversion (28) and the photon number probability:

$$P_N (t) = \sum_{\sigma=g_1,g_2,e} \langle \sigma, N || \Psi (t) \rangle \langle \Psi (t) | \sigma, N \rangle. \qquad (38)$$

In Fig. 2, the photon number probability $P_N (t)$ is shown as a function of scaled time t/T (where $T = 2\pi/\omega$ is the mode period) for the two-and three-photon resonances. For the initial state, we assume the qutrit to be in the excited state and the field in vacuum state, $|e\rangle \otimes |0\rangle$. As can be seen from Fig. 2, due to the permanent dipole moment, multiphoton Fock states are excited. Figure 3 displays collapse and revival of the multiphoton Rabi oscillations. Here, the qutrit population inversion is shown with the field initially in a coherent state with two-, three-, and four-photon resonances for different mean photon numbers. As is seen from these figures, the numerical simulations are in agreement with analytic treatment in the multiphoton resonant approximation and confirm the revealed physical picture described above.

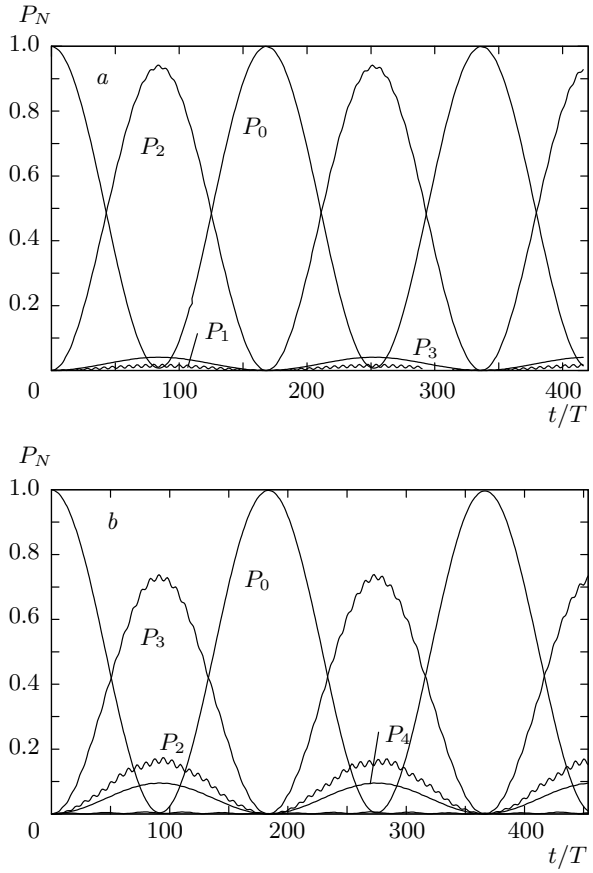

Fig. 2. Photon number probability $P_N (t)$ as a function of the scaled time at (a) two-photon and (b) three-photon resonances. Here, $\mu/\omega = 0.1$ (a), 0.2 (b) and the detuning is taken to be $\delta_2/\omega = -0.073$ (a), 0.065 (b)

We have also examined the consequence of the collapse and revival of the multiphoton Rabi oscillations on the statistical properties of the photons. For this propose, we calculated Mandel's Q-factor defined as [6]

$$Q = \frac{\overline{N^2} - \overline{N}^2 - \overline{N}}{\overline{N}}. \qquad (39)$$

The statistics is sub-Poissonian for $-1 \leq Q < 0$, super-Poissonian for $Q > 0$, and $Q = 0$ corresponds to the Poisson statistics that occurs for coherent states. As is seen from Fig. 4, during the collapse and revival of the multiphoton Rabi oscillations, the antibunching ($Q < 0$) of photons takes place.

To conclude, note that we here consider the coherent interaction of an artificial atom with cavity photons, which is correct only for the times $t < \tau_{min}$, where τ_{min} is the minimum of all relaxation times. For the considered setup, there are three types of relaxation

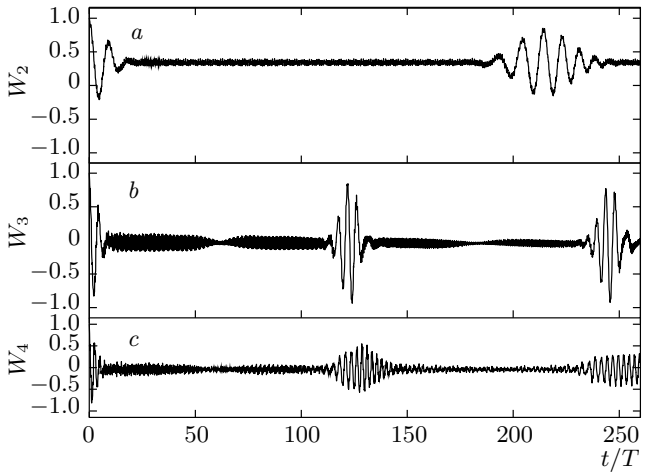

Fig. 3. Collapse and revival of the multiphoton Rabi oscillations. Population inversion of a three-level system with the photonic field initially in a coherent state is shown. (a) Two-photon resonance with the coupling parameter $\mu/\omega = 0.1$ and the mean photon number $\overline{N} = 20$. (b) Three-photon resonance with$\mu/\omega = 0.2$ and the mean photon number $\overline{N} = 30$. (c) Four-photon resonance, but for $\mu/\omega = 0.25$ and $\overline{N} = 50$

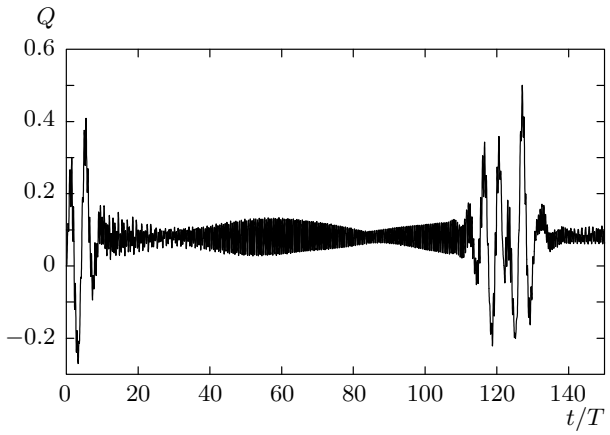

Fig. 4. Mandel's Q-factor versus the scaled time for the setup in Fig. 3b

processes that need to be considered. The first process is the loss of photons from the resonator at a rate $\kappa = \omega/Q_l$, where Q_l is the loaded quality factor of the cavity. The typical values of Q_l for high-quality cavities are $Q_l = 10^5$–10^6 [3, 10, 29, 30]. Therefore, the average photon lifetime in the cavity, $1/\kappa$, exceeds $10^4 T$. The next two processes are the energy relaxation and state dephasing of the artificial atom. Dephasing is usually the dominant mechanism for relaxation. The dephasing time T_φ depends on the experimental conditions. Recent advances in this field [30] make superconducting qubits available with the coherence time approaching 10^5 ns. Even for moderate values $T_\varphi \approx 100$ ns, in the frequency range $\omega/2\pi \approx 10$ GHz, one can coherently manipulate with artificial atoms on time scales of $10^3 T$. This is sufficient for the multiphoton Rabi oscillations considered above.

4. CONCLUSION

We have presented a theoretical treatment of the quantum dynamics of a qutrit in a polar-Λ configuration interacting with a single-mode photonic field in the ultrastrong coupling regime. For the ultrastrong couplings, we have solved the Schrödinger equation in the multiphoton resonant approximation and obtained simple analytic expressions for the eigenstates and eigenenergies. For the n-photon resonance, we then have entangled states of a qutrit and position-displaced Fock states. We have also investigated the temporal quantum dynamics of the considered system at the multiphoton resonance and showed that due to the permanent dipole moments in the lower states, Rabi oscillations of population inversion are possible with a periodic multiphoton exchange between the qutrit and the photonic field. For the quantized field prepared initially in a coherent state, the collapse/revival of multiphoton Rabi oscillations and photon antibunching occur. The obtained results are also applicable to atoms with the Γ configuration, which is unitarily equivalent to the polar-V configuration. The proposed model may have diverse applications in QED with artificial atoms, especially, in the circuit QED where the considered qutrit configuration and ultrastrong coupling regime are achievable.

This paper was supported by State Committee of Science, Republic of Armenia (Project No. 13RF-002) and the RFBR (Project No. 13-02-90600).

APPENDIX

Implementation of a polar-Λ system and its equivalence to the L configuration

Here, we outline how to implement a polar-Λ system in circuit QED. Then we prove the equivalence of the polar-Λ and L configurations. As an illustrative physical system, we consider a three-Josephson-junction loop [26, 27]. For a superconducting loop that contains three Josephson junctions (with the Josephson energies $E_{J1} = E_{J2} = E_J$, $E_{J3} = \alpha E_J$) and with

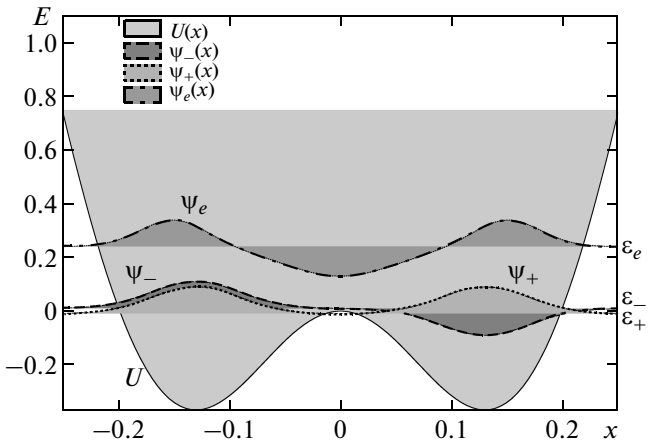

Fig. 5. Cut along the $\phi_p = 0$ axis of the double well potential $U(x) \equiv U_J(0, 2\pi x)$ (solid bold line) with the first, Ψ_+ (dotted line), second, Ψ_- (dashed line), and third, Ψ_e (dash-dotted line), eigenstates. Here, $f = 1/2$, $\beta_L = 0.5$, $\alpha = 0.8$, and the energy E is in units of E_J and is measured from the local maximum of $U(x)$

an external magnetic flux Φ_e piercing the loop, the effective potential landscape can be represented as [27]

$$U_J(\varphi_p, \varphi_m) = E_J \left[2 + \alpha - 2\cos\phi_p \cos\phi_m - \right.$$
$$\left. - \alpha \cos\left(2\pi f + \frac{2\pi L I}{\Phi_0} + 2\phi_m \right) \right] + \frac{1}{2} L_0 I^2. \quad \text{(A.1)}$$

Here, L_0 is the total inductance, $\Phi_0 = \pi\hbar/e$ is the flux quantum, $f = \Phi_e/\Phi_0$ is the reduced magnetic flux, and $I = (2\pi E_J/\Phi_0)\sin(\phi_p + \phi_m)$ is the supercurrent. The quantities ϕ_p and ϕ_m are phase variables. At $f = 0.5$ for the inductance ratio $\beta_L = L_0/L_J$ values from zero to one (where $L_J = (\Phi_0/2\pi)^2/E_J$ is the Josephson junction inductance), a symmetric double-well potential structure exists. In Fig. 5, we show a double-well potential $U(x) \equiv U_J(0, 2\pi x)$ with three eigenstates. As was shown in Ref. [28], the optical selection rules of microwave-assisted transitions in this potential are the same as the ones for the electric-dipole transitions for an electron in a symmetric 1D double-well potential, that is, the matrix element of the electric dipole moment is nonzero for states of different parity. For the chosen parameters, the first two eigenstates are localized in the wells of the potential, while the higher eigenstate is delocalized. The ground eigenstate is an even function, the eigenstate corresponding to the adjacent level is an odd function, and the eigenstate of the excited state is an even function. According to the selection rule, we have the L configuration and in the single-mode photonic field we can write the Hamiltonian

$$\widehat{H}_{\mathrm{L+ph}} = \hbar\omega \left(\widehat{a}^\dagger \widehat{a} + \frac{1}{2} \right) + \widehat{H}_{\mathrm{L}} +$$
$$+ \epsilon d_{+-} \widehat{S}_{+\leftrightarrow -} \left(\widehat{a}^\dagger + \widehat{a} \right) + \epsilon d_{-e} \widehat{S}_{-\leftrightarrow e} \left(\widehat{a}^\dagger + \widehat{a} \right), \quad \text{(A.2)}$$

where

$$\widehat{H}_{\mathrm{L}} = \begin{pmatrix} \varepsilon_+ & 0 & 0 \\ 0 & \varepsilon_- & 0 \\ 0 & 0 & \varepsilon_e \end{pmatrix}, \quad \text{(A.3)}$$

d_{+-} and d_{-e} are transition dipole moments, $\epsilon\left(\widehat{a}^\dagger + \widehat{a}\right)$ is the "electric field" operator, and

$$\widehat{S}_{+\leftrightarrow -} = \begin{pmatrix} 0 & 1 & 0 \\ 1 & 0 & 0 \\ 0 & 0 & 0 \end{pmatrix},$$
$$\widehat{S}_{-\leftrightarrow e} = \begin{pmatrix} 0 & 0 & 0 \\ 0 & 0 & 1 \\ 0 & 1 & 0 \end{pmatrix} \quad \text{(A.4)}$$

are transition operators. We now apply the unitary transformation $(\widehat{U}\widehat{F}\widehat{U}^\dagger)$ with

$$\widehat{U} = \frac{1}{\sqrt{2}} \begin{pmatrix} 1 & -1 & 0 \\ 1 & 1 & 0 \\ 0 & 0 & \sqrt{2} \end{pmatrix}. \quad \text{(A.5)}$$

For the transformed operators, we obtain

$$\widehat{H}'_L = \begin{pmatrix} \dfrac{\varepsilon_+ + \varepsilon_-}{2} & \dfrac{\varepsilon_+ - \varepsilon_-}{2} & 0 \\ \dfrac{\varepsilon_+ - \varepsilon_-}{2} & \dfrac{\varepsilon_+ + \varepsilon_-}{2} & 0 \\ 0 & 0 & \varepsilon_e \end{pmatrix}, \quad \text{(A.6)}$$

$$\widehat{S}'_{+\leftrightarrow -} = \begin{pmatrix} -1 & 0 & 0 \\ 0 & 1 & 0 \\ 0 & 0 & 0 \end{pmatrix} \equiv \widehat{S}_L, \quad \text{(A.7)}$$

$$\widehat{S}'_{-\leftrightarrow e} = -\frac{1}{\sqrt{2}} \begin{pmatrix} 0 & 0 & 1 \\ 0 & 0 & -1 \\ 1 & -1 & 0 \end{pmatrix} \equiv -\frac{1}{\sqrt{2}} \widehat{S}_t. \quad \text{(A.8)}$$

It is easy to see that the transformed Hamiltonian corresponds to the polar-Λ configuration considered in this paper (see Eq. (2)) with the parameters

$$\varepsilon_g = \frac{\varepsilon_+ + \varepsilon_-}{2}, \quad \Delta = \frac{\varepsilon_+ - \varepsilon_-}{2};$$
$$\mu = \frac{\epsilon d_{+-}}{\hbar}, \quad \lambda = -\frac{1}{\sqrt{2}} \frac{\epsilon d_{-e}}{\hbar}. \tag{A.9}$$

For the setup in Fig. 5, $|\varepsilon_e - \varepsilon_g| / \Delta \approx 25$, and $|\mu/\lambda| \approx \approx 5.75$. The terms $\widehat{S}_L$ and $\widehat{S}_t$ describe electric-dipole-moment matrix elements. The diagonal elements are the permanent dipole moments and are described by the terms proportional to $\widehat{S}_L$. This is also obvious in the coordinate picture for an electron in a symmetric 1D double-well potential. If the probability of the tunnel transition between the "left" and "right" potential wells is small ($|\Delta| \ll |\varepsilon_e - \varepsilon_g|$), we have a nearly degenerate ground state, and can therefore use two equivalent bases. In the L configuration, the two lowest-energy eingenstates are $|\pm\rangle = (|\text{left}\rangle \pm |\text{right}\rangle) / \sqrt{2}$, where $|\text{left}\rangle$ and $|\text{right}\rangle$ are the basis wave functions in the polar-Λ configuration and represent the situations where the particle is in the left or right potential well with the opposite permanent dipole moments.

REFERENCES

1. H. I. Yoo and J. H. Eberly, Phys. Rep. **118**, 239 (1985).
2. B. W. Shore and P. L. Knight, J. Mod. Opt. **40**, 1195 (1993).
3. J. M. Raimond, M. Brune, and S. Haroche, Rev. Mod. Phys. **73**, 565 (2001).
4. E. T. Jaynes and F. W. Cummings, Proc. IEEE **51**, 89 (1963).
5. C. V. Sukumar and B. Buck, Phys. Lett. A **83**, 211 (1981).
6. L. Mandel and E. Wolf, *Optical Coherence and Quantum Optics*, Cambridge Univ. Press, Cambridge (1995).
7. M. O. Scully and M. S. Zubairy, *Quantum Optics*, Cambridge Univ. Press, Cambridge (1997).
8. M. A. Nielsen and I. L. Chuang, *Quantum Computation and Quantum Information*, Cambridge Univ. Press, Cambridge (2010).
9. K. Hennessy et al., Nature **445**, 896 (2007).
10. A. Wallraff et al., Nature **431**, 162 (2004).
11. O. V. Kibis, Phys. Rev. B **81**, 165433 (2010).
12. D. Bruß and C. Macchiavello, Phys. Rev. Lett **88**, 127901 (2002).
13. H. K. Avetissian and G. F. Mkrtchian, Phys. Rev. A **66**, 033403 (2002).
14. H. K. Avetissian, B. R. Avchyan, and G. F. Mkrtchian, Phys. Rev. A **74**, 063413 (2006).
15. T. Niemczyk et al., Nature Phys. **6**, 772 (2010).
16. C. Ciuti, G. Bastard, and I. Carusotto, Phys. Rev. B **72**, 115303 (2005).
17. C. M. Wilson et al., Nature **479**, 376 (2011).
18. R. Stassi, A. Ridolfo, O. Di Stefano et al., Phys. Rev. Lett. **110**, 243601 (2013).
19. S. Ashhab and F. Nori, Phys. Rev. A **81**, 042311 (2010).
20. O. V. Kibis, Phys. Rev. Lett. **107**, 106802 (2011).
21. T. Espinosa-Ortega, O. Kyriienko, O. V. Kibis, and I. A. Shelykh, Phys. Rev. A **89**, 062115 (2014).
22. H. K. Avetissian and G. F. Mkrtchian, Phys. Rev. A **88**, 043811 (2013).
23. H. Walther, B. T. H. Varcoe, B. G. Englert, and T. Becker, Rep. Prog. Phys. **69**, 1325 (2006).
24. A. J. Leggett, S. Chakravarty, A. T. Dorsey et al., Rev. Mod. Phys. **59**, 1 (1987).
25. R. Rouse, S. Han, and J. E. Lukens, Phys. Rev. Lett. **75**, 1614 (1995); J. R. Friedman, V. Patel, W. Chen et al., Nature **406**, 43 (2000).
26. J. E. Mooij, T. P. Orlando, L. Levitov et al., Science **285**, 1036 (1999).
27. J. Q. You, Y. Nakamura, and F. Nori, Phys. Rev. B **71**, 024532 (2005).
28. Y.-x. Liu, J. Q. You, L. F. Wei et al., Phys. Rev. Lett. **95**, 087001 (2005).
29. H. Paik et al., Phys. Rev. Lett. **107**, 240501 (2011).
30. C. Rigetti et al., Phys. Rev. B **86**, 100506(R) (2012).